

Electronic structure of Sn₂S₃ compound with the mixed valency of tin

M. M. BLETSKAN*, D. I. BLETSKAN

Uzhgorod National University, Department of Physics, 88000 Uzhgorod, Voloshyn str., 54, Ukraine

The energy band structure, total and local partial densities of states, a spatial distribution of electron charge density of Sn₂S₃ have been calculated by a density functional method. From the data of a band structure calculation follow that Sn₂S₃ is an indirect semiconductor with the calculated width of forbidden gap $E_{gi} = 0.53$ eV. The calculated total density of states along the all Brillouin zone in a valence band of Sn₂S₃ crystal is compared to X-ray photoelectron spectrum (XPS), and the partial density of S3p-states has been correlated with X-ray emission spectrum (XES). Theoretically calculated energy distribution of the total and partial densities of states qualitatively and quantitatively represent the main observational features of XPS and XES spectra.

(Received July 16, 2013; accepted May 15, 2014)

Keywords: Tin sesquisulfide, Electronic structure, Density of states, Lone pair

1. Introduction

According to the studies of phase equilibria in the Sn–S system, there are three basic compounds: tin monosulfide (SnS), tin disulfide (SnS₂) and tin sesquisulfide (Sn₂S₃), in which tin atoms have various valency (an oxidation state) [1, 2]. Unlike to the binary compounds SnS and SnS₂, in which tin atoms have II and IV valence, respectively, Sn₂S₃ relates to compounds with the mixed valence of tin and their crystal structure contains equal quantity of two- and tetravalent tin atoms [3–5].

The crystals and thin layers of tin sulphides have become the objects of intensive experimental studies related to the new opportunities of these compounds application for a creation on their basis the solar cells [6], Schottky barriers [7], photovoltaic detectors [8], detectors and generators of infrared radiation on the basis of Sn₂S₃/CdTe- and Sn₂S₃/GaSb-type heterostructures [9], also the heterostructures by landing to optical contact [10], as the electrode materials of lithium-ion batteries [11], that stimulates further studying of their physical properties.

Among the known tin sulphides the most studied are tin monosulfide and tin disulfide, while Sn₂S₃ crystals and thin layers are still studied very poorly. The literature contains only information about the study of electrical conductivity and the fundamental absorption edge [9, 12], Raman scattering spectra and IR reflection spectra [13–15], thermodynamic properties [16], Mossbauer spectra [17, 18], also X-ray photoelectron (XPS) and emission (XES) spectra of Sn₂S₃ [19, 20].

We have no any calculation data on the electronic structure of Sn₂S₃, except the total and partial densities of states [21], although it is well known, that the electronic structure of $E(\mathbf{k})$ is one of the fundamental characteristics which largely determines the basic properties of crystals.

Therefore the theoretical studying of electronic structure and the charging state in the crystal is interesting, because received information will be useful for the spectroscopic research interpretation.

In this paper the band structure, total and local partial density of electronic states, the spatial distribution of electron valence charge density of Sn₂S₃ crystal have been calculated using a nonempirical *ab initio* density functional method.

2. Crystal structure of Sn₂S₃

The electron configuration of valence states of insulated tin atoms is $4d^{10}5s^25p^2$ and of sulphur ones – $3s^23p^4$. Sulphur is more electronegative element in tin monosulfide and, therefore, it takes two electrons from the tin atom, that leads to $3s^23p^6$ electron configuration for S and $4d^{10}5s^25p^0$ one for Sn. Thus, the oxidation degree of a cation in tin monosulfide is equal II. In Sn^{II}-state two 5p-electrons are involved in a chemical bond forming, while two 5s-electrons generate the lone pair. This pair does not directly involve in the chemical bonding, but it significantly affects on non-symmetric location of sulphur atoms around the tin atom, which leads to a generation of the deformed ψ -octahedra [SnS₅•E•], where •E• is electronic lone pair. In the tin disulfide, which crystal structure is built from the regular octahedra [SnS₆], the tin oxidation degree is IV.

Sn₂S₃ compound with the mixed valency of tin (Sn^{II}Sn^{IV}S₃) obtain by the direct fusion of the equimolar quantities mixture of SnS₂ and SnS at the ~1079 °K temperature. Tin sesquisulfid crystallizes in orthorhombic structure (Fig. 1, a) which symmetry is described by the spatial group $D_{2h}^{16}(Pnma)$, with lattice parameters: $a = 8.878$, $b = 3.751$ and $c = 14.020$ Å, Z=4 [3–5].

The crystal structure of Sn_2S_3 is built from the deformed octahedra $[\text{Sn}^{\text{IV}}\text{S}_6]$, linked by the common edges in the endless dual chains, which stretch along the b -axis. The ψ -tetrahedra $[\text{Sn}^{\text{II}}\text{S}_3\text{E}\cdot]$ abut to the dual chains on both sides, whereby the endless ribbons are formed. The ion-covalent type of bonding acts inside the ribbons, and the bond between ribbons is carried out by weak Van-der-Waals forces.

Sn_2S_3 unit cell contains twenty atoms, of which four are Sn^{II} , four – Sn^{IV} and twelve – S (Fig.2). There are nonequivalent positions of Sn^{II} and Sn^{IV} atoms in the crystal lattice. Bivalent Sn^{II} and tetravalent Sn^{IV} , as well as three atoms of sulphur S(1), S(2) and S(3) occupy five different $4c$ -positions of the spatial group $Pnma$ with the point symmetry m (Fig. 1, Table. 1).

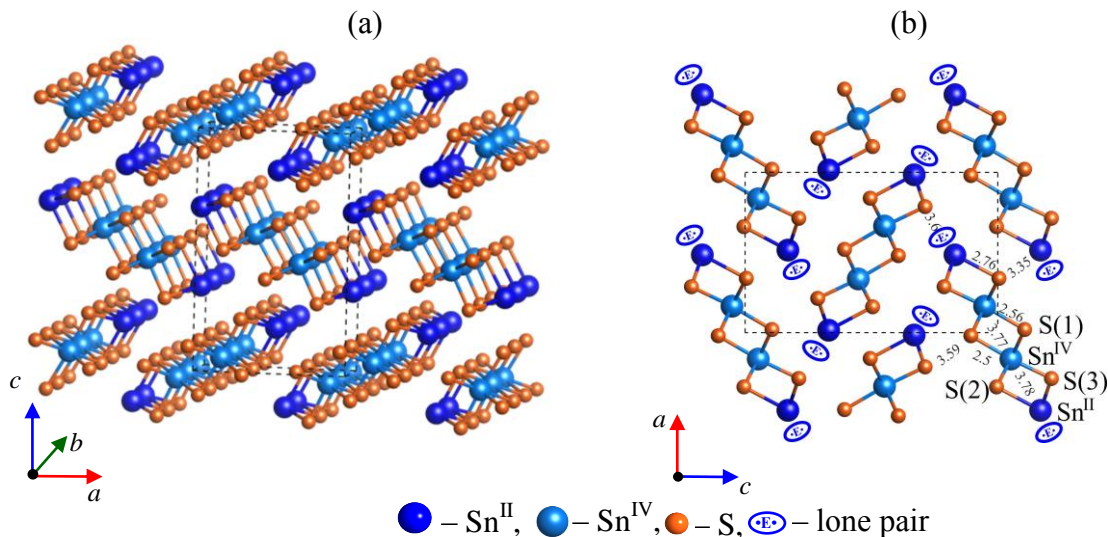


Fig. 1. The crystal structure (a) and the projection of crystal structure on XZ plane (b) of orthorhombic Sn_2S_3 .

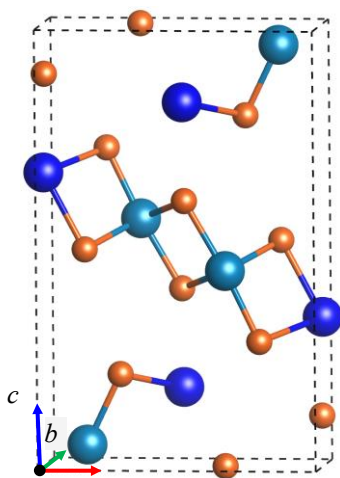


Fig. 2. The elementary cell of orthorhombic Sn_2S_3 .

3. Calculation method

Energy band structure calculations are performed within the electron density functional theory using the plane-wave basis set (ABINIT), localized atomic orbitals and norm-conserving pseudopotentials (SIESTA) realized in software packages [22–25], which carried out a pseudopotential formalism of the electron density functional [26, 27]. The first-principles atomic norm-conserving pseudopotentials [28] were used in calculations for the electron configurations: for Sn atoms – $[\text{Kr}] 5s^2 5p^2$, for S atoms – $[\text{Ne}] 3s^2 3p^4$. The indicated states belong to

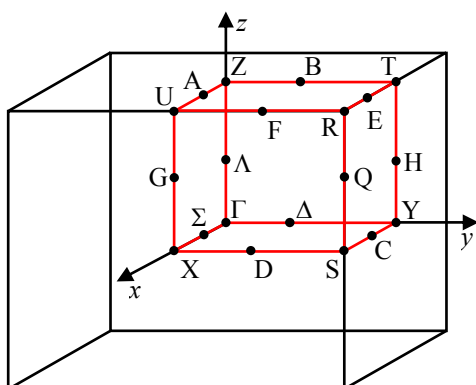
the valence shells, $[\text{Kr}]$, $[\text{Ne}]$ – to the core. The exchange-correlation interaction was considered in the local electron density approximation [29] and the generalized gradient approximation [30]. Calculations were performed for the optimized structure with the relaxed parameters given in Table 1.

4. Results and their discussion

4.1. Band structure and the density of electron states

The electronic band structure calculations were carried out in the high-symmetry points and directions of the Brillouin zone of the orthorhombic lattice (Fig. 3). The electronic band structure of Sn_2S_3 is given in Fig. 4 where zero of energy taken as the last occupied state.

The energy spectrum $E(\mathbf{k})$ of tin sesquisulfide valence bands consists of 52 dispersive branches which grouped into three subbands (Fig. 5). It follows from the analysis of energy distribution of local partial density of states for tin and sulphur that s -, p - and d -states give different contributions, which differ in size, into each of three subbands. The maximum values density of states of sulphur and tin d -electrons are essentially smaller than the maximum values density of s - and p -states, therefore they do not essentially affect on the form of Sn_2S_3 total density of states (Fig. 5). The greatest statistical weight in Sn_2S_3 electronic structure have S $3s$ -states, formed the lowest occupied subbands, and S $3p$ -states, which formed the middle and the highest occupied valence bands.

Fig. 3. The Brillouin zone of orthorhombic Sn₂S₃.

For more detailed nature determination of the occupied bands we would use the results of tin partial density of states calculations with II and IV valences, shown in Fig. 5. It is clear from this Figure that Sn^{IV} 5s-states give the negligible contribution to the lowest band of S 3s- occupied states ($-14.58 \div -12.07$ eV) into full subband and Sn^{IV} 5p-states only in its top part. The middle bunch of eight valence bands ($-8.43 \div -5.24$ eV) is separated from S 3s-bands by the forbidden gap of 3.64 eV and it formed by sulphur 3p-states and tin 5s-states. Besides, the contribution of Sn^{IV} 5s-states prevails in the lower part of this band, and in the highest part – Sn^{II} 5s-states of the lone pair.

Table 1. Crystal structure data of Sn₂S₃ compound.

Compound	Crystal system, Spatial group, Number of formula units	Elementary cell parameters, Å	Atomic coordinates				Wyckoff position	References
			Atom	x	y	z		
Sn ₂ S ₃	Orthorhombic, $D_{2h}^{16}, Pnma$, Z = 4	$a = 8.878$ $b = 3.751$ $c = 14.02$	Sn ^{IV}	0.16494	0.25	0.05195	4c	[5]
			Sn ^{II}	0.48509	0.75	0.16936	4c	
			S1	-0.01953	0.75	0.10640	4c	
			S2	0.33879	0.75	-0.00476	4c	
			S3	0.28631	0.25	0.21246	4c	
		$a = 8.57829$ $b = 3.81088$ $c = 13.80329$	Sn ^{IV}	0.172285	0.25	0.053323	4c	LDA optimization
			Sn ^{II}	0.509729	0.75	0.172283	4c	
			S1	0.981711	0.75	0.110121	4c	
			S2	0.352714	0.75	0.992489	4c	
			S3	0.299370	0.25	0.217827	4c	
		$a = 8.59211$ $b = 3.86640$ $c = 13.91800$	Sn ^{IV}	0.17394	0.25	0.05409	4c	GGA optimization
			Sn ^{II}	0.51723	0.75	0.17367	4c	
			S1	0.98151	0.75	0.11069	4c	
			S2	0.35557	0.75	0.99234	4c	
			S3	0.30237	0.25	0.21911	4c	

From the calculations of Sn₂S₃ electronic structure (Fig. 4) follows that the top of valence band is localized at Σ direction of the Brillouin zone, and the bottom of conductivity band is at U point. Thus, the orthorhombic tin

sesquisulfide is the indirect-gap semiconductor with the calculated forbidden band width $E_{gi} = 0.53$ eV (transition $\Sigma \rightarrow U$). The first direct transition is in Z point ($E_{gd} = 0.54$ eV).

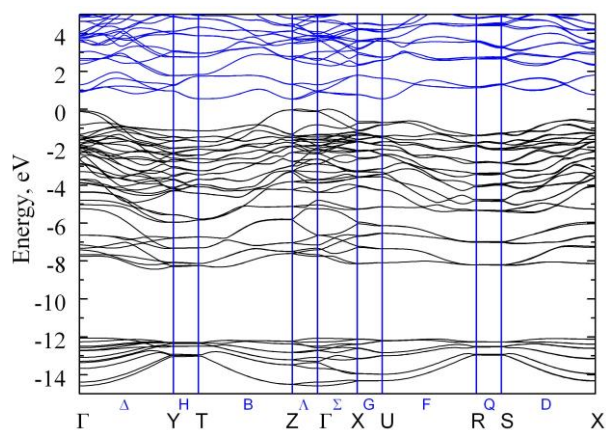


Fig. 4. Band structure of Sn_2S_3 .

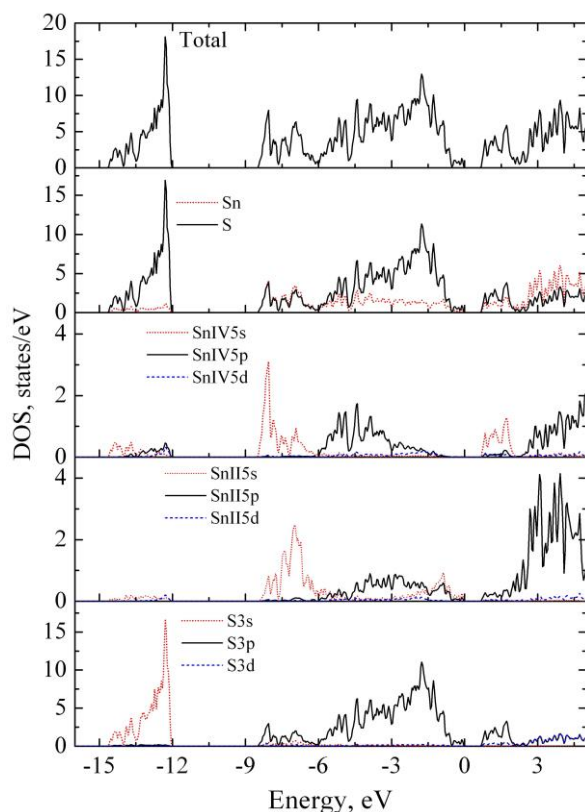


Fig. 5. The total and local partial densities of states of Sn_2S_3 .

4.2. The comparison of theory and experiment

Reliable information about the crystal band structures can be received by the comparison of theoretically calculated total and partial density of states with the experimental X-ray photoelectron and emission spectra which reflect the features of electronic states energy distribution in the valence band [31].

The experimental studies of valence band density of states for Sn_2S_3 crystals were performed by the authors [19]. It was performed two types of photoemission

experiments. The ordinary X-ray photoelectron spectra excited by photon quanta with the energy of $h\nu = 1253.6$ eV and X-ray emission spectra of sulphur 3p-states were measured.

In Fig. 6 the theoretically calculated total and the local partial S 3p- densities of states compared to the experimental X-ray photoelectron spectra and the emission K-spectra of sulfur for Sn_2S_3 crystal taken from the work [19] in an uniform energy scale. The comparison of theoretical and experimental energy spectra was carried out by the main maximum. Evidently, that the energy positions and the structure of main features of the calculated total density of states are in a good agreement with the experiment. The analysis of local partial densities of states, given in Fig. 5, allows revealing the nature of photoelectron spectra maxima. Thus, D maximum near the bottom of Sn_2S_3 valence band is caused mainly by 3s-states of sulphur, and hybridized 5s-states of tin, also 3p-states of sulphur form a doublet C i C', and besides in maximum C' the main contribution bring Sn^{IV} 5s-states, and in maximum C – Sn^{II} 5s-states. Maximum B' is created by hybridized S 3p- and Sn^{IV} 5p-states, and B one – by S 3p- and Sn^{II} 5p-states. The most intensive peak A is formed mainly by 3p-states of sulphur with a small impurity of 5s- and 5p-states of divalent tin.

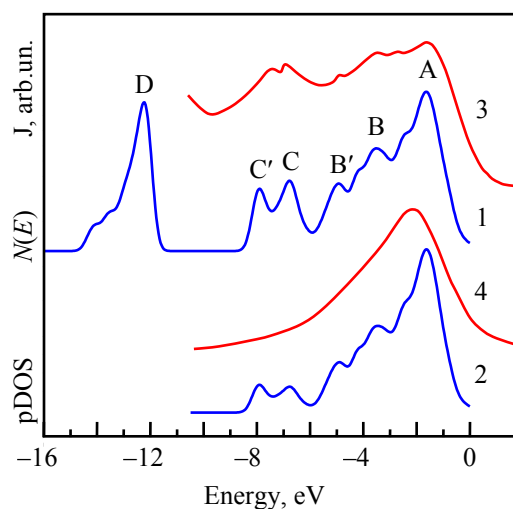


Fig. 6. The calculated total $N(E)$ (1) and S 3p- local partial (2) densities of states, and experimental XPS (3) and S 3p- XES (4) Sn_2S_3 spectra [19].

4.3. The spatial distribution of valence charge

Since the lone electron pair of bivalent tin Sn^{II} is involved in Sn_2S_3 crystal structure formation, it is important to visualize it, which can be accomplished using the bulk distribution of charge density (Fig. 7). An isosurface distribution form $\rho(r)$ in the endless ribbons shows the formation of strong interatomic interactions between Sn and S atoms inside the ribbon and the

existence of a weak interaction between atoms of the neighbor ribbons, occurred with the assistance of lone pair of Sn^{II} atom.

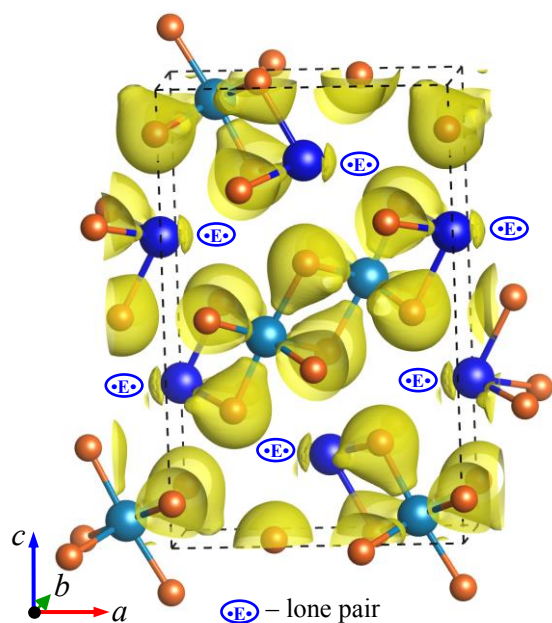


Fig. 7. The spatial distribution of the valence charge bulk density in Sn_2S_3 crystal.

Fig. 7 shows, that the charging (electron) density is concentrated mainly within $[\text{SnS}_6]$ octahedra and ψ -tetrahedra $[\text{SnS}_3\cdot\text{E}\cdot]$, which form the endless ribbons. In the octahedra and tetrahedra the isosurfaces $\rho(r)$ are strongly deformed along the directions of Sn–S bonds.

The distribution of electrons in Sn_2S_3 crystal can also be described by the electron density charge maps, which are presented for four planes in Fig. 8. The electron density maps show that the electron density distribution in Sn_2S_3 crystal is anisotropic: there is a strong ion-covalent bond between tin and sulphur ions in octahedra $[\text{Sn}^{\text{IV}}\text{S}_6]$ and ψ -tetrahedra $[\text{Sn}^{\text{II}}\text{S}_3\cdot\text{E}\cdot]$ in the endless ribbons; at the same time the ions belonging to two different ribbons interact extremely weakly.

The contours, which represent the charge on Sn–S bonds in ψ -tetrahedra $[\text{Sn}^{\text{II}}\text{S}_3\cdot\text{E}\cdot]$ and octahedra $[\text{Sn}^{\text{IV}}\text{S}_6]$, that belong to the same ribbon (Fig. 7, 8), are well localized and have an egg form. The high concentration of electrons near the localization places of S and Sn atoms are the contours of the core electrons contribution. Whereas in Sn_2S_3 the core ions of Sn have charge +2 and +4, and S ones – +6, it leads to the appearance of the ionic component of chemical bond. The ionic bond is characterized by the increasing of charge around the anion and decreasing of charge on the covalent bond between the ions which clearly illustrated by the electron density maps in Fig. 8. The presence of covalent bond is responsible for the stability of octahedral-tetrahedral structure for this compound.

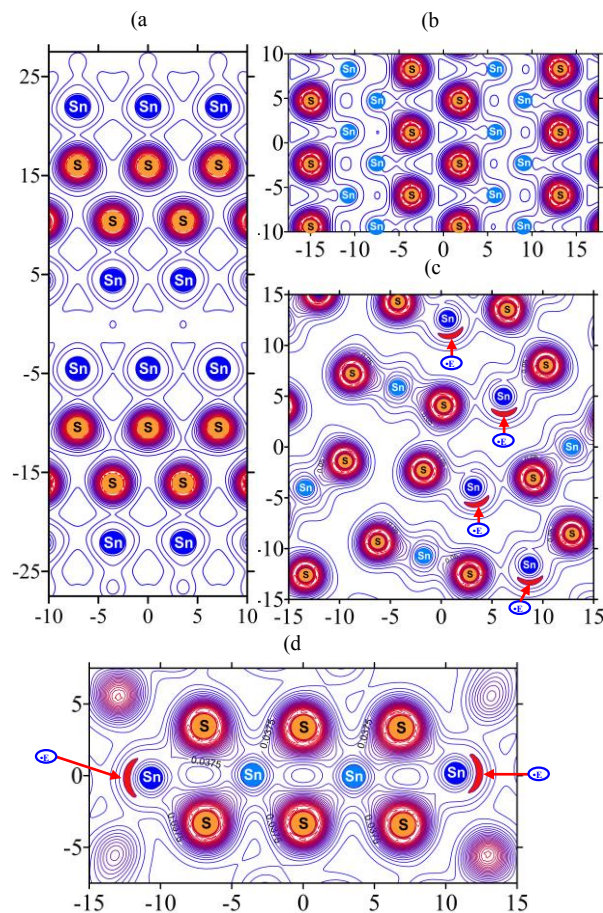


Fig 8. The maps of the valence charge density spatial distribution of Sn_2S_3 crystal presented in the planes: a – (100), b – (001), c – (010), d – through atoms of tin in the ribbon.

5. Conclusions

For the first time the band electronic structure calculations, the total and the local partial density of electronic states, also the spatial distribution of electron valence charge density of tin sesquisulfide have been performed by the electron density functional technique. It is shown that Sn_2S_3 is the indirect semiconductor with the calculated band gap of $E_{\text{gi}} = 0.53$ eV (transition $\Sigma \rightarrow \text{U}$).

The form, location and nature of bands in Sn_2S_3 electronic energy spectrum are in good agreement with the data of photoemission spectroscopy, which confirms the correctness of the executed electronic structure calculations.

The analysis of charge density spatial distribution shows the presence of ion-covalent component of bonds within the endless ribbons formed by coordinational octahedra $[\text{Sn}^{\text{IV}}\text{S}_6]$ and ψ -tetrahedra $[\text{Sn}^{\text{II}}\text{S}_3\cdot\text{E}\cdot]$, and the interaction between the ribbons is caused by Van-der-Waals forces with participation of the lone electronic pair. The visualization of lone pair of Sn^{II} 5s-electrons in Sn_2S_3 crystal structure by the construction of 2D and 3D distributions of the electron valence charge density was carried out.

References

- [1] M. I. Karakhanova, A. S. Pashinkin, A. V. Novoselova, *Izv. Akad. Nauk SSSR Neorg. Mater.*, **3**, 1979 (1967).
- [2] G. H. Moh. N. Jb. Miner. Abh., **111**, 227 (1969).
- [3] D. Mootz, R. Kunzmann, *Acta. Cryst.*, **15**, 913 (1962).
- [4] D. Mootz, H. Puhl, *Acta. Cryst.*, **23**, 471 (1967).
- [5] R. Kniep, D. Mootz, U. Severin, H. Wunderlich, *Acta Cryst. B*, **38**, 2022(1982).
- [6] P. D. Antunez, J. J. Buckley, R. L. Brutchey, *Nanoscale.*, **3**, 2399 (2011).
- [7] C. Clemen, X. I. Saldana, P. Munz, E. Bucher, *Phys. Stat. Sol. (a)*, **49**, 437 (1978).
- [8] D. Trbojevic, P. M. Nikolic, B. Perovic, V. Cvekic, *Appl. Phys. Lett.*, **38**, 362 (1981).
- [9] M. Khadraoui, N. Benramdane, C. Mathieu, A. Bouzidi, R. Miloua, Z. Kebbaba, K. Sahraoui, R. Desfeux, *Sol. State. Commun.*, **150**, 297 (2010).
- [10] V.N. Katerinchuk, M.Z. Kovalyuk. *J. Advanced Materials.*, **4**, 40(1997).
- [11] J. Morales, C. Perez-Vicente, J.L. Tirado. *Solid State Ionics.*, **51**, 133 (1992).
- [12] U. V. Alpen, J. Fenner, E. Mater. Res. Bull., **10**, 175 (1975).
- [13] H. R. Chandrasekhar, D. G. Mead, *Phys. Rev. B*, **19**, 932 (1979).
- [14] D. G. Mead, H. R. Chandrasekhar, *Infrared Physics.*, **20**, 245 (1980).
- [15] L. S. Price, I. P. Parkin, A. M. E. Hardy, R. J. H. Clark, T. G. Hibbert, K. C. Molloy, *Chem. Mater.*, **11**, 1792 (1999).
- [16] H. Wiedemeier, F. J. Csillag, *Z. anorg. Und allg. Chem.*, **469**, 197 (1980).
- [17] S. Ichiba, M. Katada, H. Negita, *Chemistry Letters*, **3**, 979 (1974).
- [18] G. Amthauer, J. Fenner, S. Hafner, W. B. Holzapfel, R. Keller, *J. Chem. Phys.*, **70**, 4837 (1979).
- [19] A. G. De La Rocque, E. Belin-Ferré, M. F. Fontaine, C. Senemaud, J. Olivier-Fourcade, J. C. Jumas, *Phil. Mag. B*, **80**, 1933 (2000).
- [20] M. Cruz, J. Morales, J. P. Espinos, J. Sanz, *J. Sol. St. Chem.*, **175**, 359 (2003).
- [21] I. Lefebvre, M. Lannoo, J. Olivier-Fourcade, J. C. Jumas, *Phys.Rev B*, **44**, 1004 (1991).
- [22] <http://www.abinit.org/>
- [23] X. Gonze, J.-M. Beuken, R. Caracas, F. Detraux, M. Fuchs, G.-M. Rignanese, L. Sindic, G. Verstraete, G. Zerah, F. Jollet, M. Torrent, A. Roy, M. Mikami, Ph. Ghosez, J.-Y. Raty, D.C. Allan, *Comp. Mat. Sci. B.*, **25**, 478 (2002).
- [24] J. M. Soler, E. Artacho, J. D. Gale, A. Garcia, J. Junquera, P. Ordejon, D. Sanchez-Portal, *J. Phys.: Condens. Matter.*, **14**, 2745 (2002).
- [25] <http://icmab.cat/leem/siesta/>
- [26] P. Hohenberg, W. Kohn, *Phys. Rev.*, **136**, B864 (1964).
- [27] W. Kohn, L. J. Sham, *Phys. Rev.*, **140**, A1133 (1965).
- [28] C. Hartwigsen, S. Goedecker, J. Hutter, *Phys. Rev. B.*, **58**, 3641 (1998).
- [29] D. M. Ceperley, B. J. Alder, *Phys. Rev. Lett.*, **45**, 566 (1980).
- [30] J. P. Perdew, J. A. Chevary, S. H. Vosko, K. A. Jackson, M. R. Pederson, D. J. Singh, C. Fiolhais, *Phys. Rev. B*, **46**, 6671 (1992).
- [31] A. Meisel, G. Leonhardt, R. Szargan. *X-Ray Spectra and Chemical Bonding*, *Naukova Dumka*, Kiev, 1981.

*Corresponding author: crystal_lab457@yahoo.com